International Journal of Scientific Engineering and Research (IJSER)
www.ijser.in
ISSN (Online): 2347-3878, Impact Factor (2015): 3.791

Fatigue of Rail Wheels

Ranjit Patil

FEA analyst, Pune, Maharashtra, India

Abstract: ***The analysis of rolling contact fatigue differs from the 'classic' fatigue analysis in several aspects. It is also important to summarize the studies which have been already done on rolling contact fatigue specifically related to rail wheels. The paper below gives brief idea about studies related to rolling contact fatigue calculation, damage , Dang van criteria etc.***

Keywords: Rolling contact fatigue, Dang van, rail wheels fatigue

1. Introduction

The analysis of rolling contact fatigue differs from the 'classic' fatigue analysis in several aspects:

- The rolling contact loading causes a multiaxial state of stress with out-of-phase stress components and rotating principal stress directions.

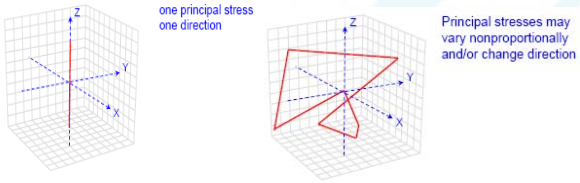

Figure 1: Multiaxial state of stress

- As they grow longer, cracks subjected to a multiaxial loading normally deviate into a Mode I dominated growth (or follow a weak path in the structure). This is not the case in rolling contact fatigue, due to the large confining pressures under the contact which normally suppresses any Mode I deformation of the crack in the absence of trapped fluids, etc. Instead cracks propagate mainly in a mixed Mode II–Mode III.

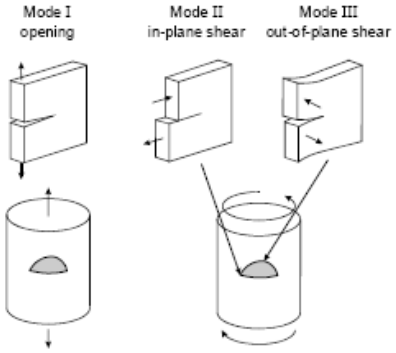

Figure 2: Modes of fracture

- In a predominantly compressive loading, the validity of traditional fatigue models may be questioned. As an illustration, Paris' law predicts zero crack growth under compressive loading in its original form since it employs the range of the Mode I stress intensity factor, the above point. Due to the compressive loading, crack face friction will control the crack propagation. The magnitude of operational crack face friction is, however, hard to quantify.
- • A similar effect of the compressive loading is that crack face deflection increases with crack length and may cause complete locking between the crack faces for part(s) of the crack .Occasional overloads may slightly accelerate crack growth, in contrast to the behavior in tensile loading. This may lead to non-conservative fatigue life predictions.

Three fairly different types of rolling contact fatigue damage in railway wheels exist
1) Surface initiated fatigue
2) Subsurface initiated fatigue
3) Fatigue initiated at deep defects

1. Surface Initiated Fatigue

Initiation of surface cracks is the result of ratcheting and/or low-cycle fatigue of the surface material. Once cracks initiate in the surface layer, they will propagate in a shallow angle to the surface, deviating first into an almost radial, and later into a circumferential direction of growth.

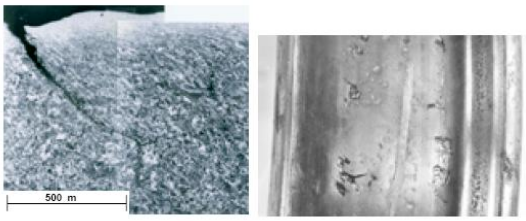

Initiation of a surface crack and the final fractured surface, from [1]

Figure 3: Surface initiated fatigue

2. Subsurface initiated fatigue

Subsurface cracks initiate at depths of below some 3 mm from the wheel tread. Below some 10 mm, the fatigue resistance will be totally governed by the presence of macroscopic inclusions. Typical features of subsurface fatigue are, no signs of macroscopic inclusions or voids at the point of fatigue initiation crack propagation in an angle downwards to a depth of some 20 mm final fracture towards the surface circumferential crack length of some 15 to 300 mm at fracture.

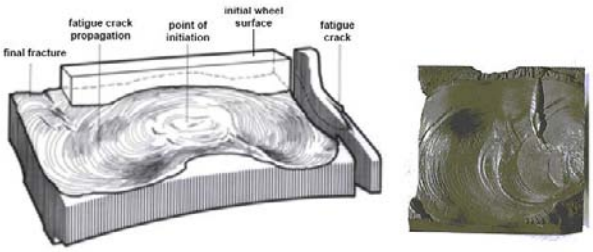

Figure 4: Subsurface initiated fatigue

3. Fatigue initiated at deep defects

The partition between 'subsurface initiated fatigue' and 'fatigue initiated at deep defects' is somewhat dim. Here, 'fatigue initiated at deep defects' denotes cracks initiated at relatively large material inclusions (in the order of 1 mm). Typical features are, fatigue crack initiation at a depth of 10–25 mm below the wheel tread crack propagation at an almost constant depth below the wheel tread (corresponding to depth of initiation) until fracture occurs final failure due to branching of the circumferentially growing crack at a length of 25 to 135 mm.

2. Literature Survey

P. J. Mutton [1] studied features associated with various forms of RCF (rolling contact fatigue) damage, identifying main characteristics responsible for initiation of fatigue crack growth.

P. J. Mutton, C. J. Epp and J. Dudek [2] studied rolling contact fatigue under axle load.They have done analysis of wheel-rail contact conditions in curved and tangent track to identify which combmations of wheel load, wheel and rail profiles result in stress levels which exceed shakedown limits

Anders Ekberg [3] discussed about initiation of fatigue cracks in the tread of a railway wheel. The division of the fatigue process into an "initiation" and a "propagation" phase is somewhat questionable since both phases may include the growth of cracks but on different scales.

G. Donzella, M. Faccoli, A. Ghidini, A. Mazz_u, R. Roberti [4] proposed model for assessing wear and rolling contact fatigue (RCF) in rails. RCF was studied taking into account different mechanisms of crack nucleation and propagation in different working conditions, and failure indexes are proposed to predict which damage mechanism prevails.

S. BogdaAski, M. Olzak, J. Stupnicki [5] presented the results of the stress analysis of rail rolling contact fatigue cracks. The basis of the model used in the analysis is the finite element approach which enables the crack tip stress environment to be described by the fracture mechanics crack tip stress intensity factors (SIFs) K,, K,,, and K,,,. The results for a semi-elliptical crack perpendicular to the rail axis and the "squat" type of crack were presented. Distributions of the SIFs along the "squat" type crack front for various locations of the wheel are also presented.

Eka Lansler, Elena Kabo [6] studied mostly about subsurface cracks in RCF.They studied deformation of such subsurface cracks under rolling contact conditions. studies are carried out with a two-dimensional elasto-plastic finite element (FE) model of a part of a wheel containing a subsurface crack.

Jonas W. Ringsberg, Torbjorn Lindba [7] They presented work is an investigation on how an initially introduced residual stress-state affects the service life of a rail, i.e. the time to fatigue crack initiation. The finite element (FE) method was used to make two-dimensional thermo-mechanical analyses of the rail cooling and roller straightening processes.

The results from the thermo-mechanical FE analyses of the rail manufacturing process showed tensile residual stresses in the longitudinal direction of the rail; this was validated with experimental measurements on newly manufactured rails.

Anders Ekberg, Elena Kabo [8] This paper gives idea about rolling contact fatigue phenomena occurring at wheels and rails is given. The paper outlines mechanisms behind the various phenomena, means of prediction, influencing parameters and possible means of prevention.

Y.B. Guo,_, Mark E. Barkey [9] They investigated the effect of process-induced residual stress on bearing rolling contact fatigue (RCF). A 2-D finite element simulation model of bearing rolling contact has been developed to incorporate the process-induced residual stress profile as initial conditions. The applied load was modeled using the interaction between the roller and the bearing inner race instead of moving elastic-based Hertzian pressure and tangential traction across the surface

Stanisław Bogdanski , Michael W. Brown [10] developed model of the fatigue behavior of three-dimensional (3D) semi-elliptical shallow-angle rolling contact fatigue (RCF) cracks by combining numerically obtained (3D FEM) linear elastic fracture mechanics (LEFM) crack front loading histories with mixed-mode fatigue crack growth rate data. The model was applied for the "squat" type of crack—typical of rail RCF failure, to predict (i) shape development, (ii) co-planar extension, (iii) spalling, and (iv) branching to transverse defects.

Anders Ekberg, Peter Sotkovszki [11] Modes of rolling contact fatigue failure were described and categorized for railway wheel treads and rims.

Jonas W. Ringsberg [12] A strategy developed for fatigue life prediction of rolling contact fatigue (RCF) crack initiation was presented. It combines elastic plastic finite element (FE) analyses, multiaxial fatigue crack initiation models used together with the critical plane concept, fatigue damage summation calculations, and comparison of results from numerical analyses and experiments

S. BogdaAski, M. Olzak, J. Stupnicki [13] They presented the results of the stress analysis of rail rolling contact fatigue cracks. The basis of the model used in the analysis was the finite element approach which enables the crack tip stress environment to be described by the fracture mechanics crack tip stress intensity factors (SIFs) K,, K,,, and K,,,. The results for a semi-elliptical crack perpendicular to the rail axis and the "squat" type of crack were presented.

A. Ekberg [14] The influence of some important parameters on the fatigue life is evaluated using the improved model. The parameters varied are vertical wheel load, diameter of wheel, radius of railhead, residual stresses, and longitudinal and transverse contact stresses.

J.W. Ringsberg , M. Loo-Morrey , B.L. Josefson , A. Kapoor , J.H. Beynon [15] In this paper they studied FE simulation of railwheel contact, fatigue crack initiation criteria for elastic shakedown, plastic shakedown and ratcheting material responses were evaluated for a pearlitic rail steel BS11 normal grade.

M.S raml , J. Flasker, I. Potrc [16] A computational numerical model for contact fatigue damage analysis of mechanical elements was presented in this paper. The computational approach is based on continuum mechanics, where a homogenous and elastic material model was assumed in the framework of the finite element method analysis. Cyclic contact loading conditions were simulated with moving Hertzian contact pressure.

Elena Kabo, Anders Ekberg [17] The influence of the size of material defects on rolling contact fatigue of railway wheels is investigated. To study differences between uniaxial tensile loading and rolling contact loading, finite element simulations of a defected component are carried out.

H. Desimone , A. Bernasconi, S. Beretta [18] They discussed about Dang-Van criteria for RCF. the problem of the calibration of the Dang Van multiaxial fatigue criterion is addressed. The discussion is based on uniaxial fatigue tests performed with different stress ratios.

Yongming Liu, Brant Stratman, Sankaran Mahadevan [19] A new multiaxial high-cycle fatigue initiation life prediction model for railroad wheels was proposed in this paper. A general fatigue damage analysis methodology for complex mechanical components was developed and applied to the wheel/rail rolling contact fatigue problem. A 3-D elasto-plastic finite element model was used for stress analysis.

Jonas W. Ringsberg, Francis J. Franklin, B Lennart Josefson, Ajay Kapoor, Jens C.O. Nielsen [20]
A systematic approach for fatigue design of surface coated rails (called two-material rails) against rolling contact fatigue was presented. It incorporates dynamic train–track interaction simulations, three-dimensional finite element (FE) calculations, shakedown theory, and lab and field trials. The approach was validated against two-dimensional twin-disc tests in laboratory, where surface coated disc specimens were used.

3. Studies related to Rolling contact fatigue

EQUIVALENT-STRESS APPROACHES IN ROLLING CONTACT FATIGUE

A (subsurface) material point in the rim of a railway wheel is indicated . During a evolution of the wheel, this material point will be subjected to a multiaxial state of stress that will vary in magnitude from almost zero (when residual stresses are excluded) to a maximum value during rail contact and then back to zero. Also, the direction of the principal stresses will vary during the load cycle.

In order to quantify the multiaxial stress field, so that material data from uniaxial testing can be exploited, a scalar equivalent-stress measure is introduced. This measure should include the influence of a superimposed hydrostatic stress and it should include no contribution from a superimposed static shear stress. The hydrostatic stress can, for instance, be included by its mean or maximum value during a stress cycle (as is the case in the Sines and Goodman criteria, respectively) or by its time dependent value (as in the present model).

When the mid-value τmid of the shear stress vector in a given plane has been defined, an equivalent-stress criterion can be formulated. The current magnitude, or "amplitude", τa(t)of the local shear stress i.e. the current value minus the mid-value during a stress cycle, is calculated as , τa(t) = τi(t) - τmid ì where τi(t) is the shear stress vector at time *t.* According to the criterion used in the present model, damage occurs if the combination of the current "amplitude" τa(t) and the current value σh(t) of the hydrostatic stress (positive when tensile) at the material point considered, fulfils the following inequality during some time portions of the full stress cycle

$$\tau_{EQ} = \tau_a(t) + a_{DV}\sigma_h(t) > \tau_e \quad \text{----------(1)}$$

where,

τ_e = is a material parameter (positive) usually taken equal to the fatigue limit of the material in pure shear

a_{DV} = is a dimensionless material parameter (positive) representing the influence of the hydrostatic stress

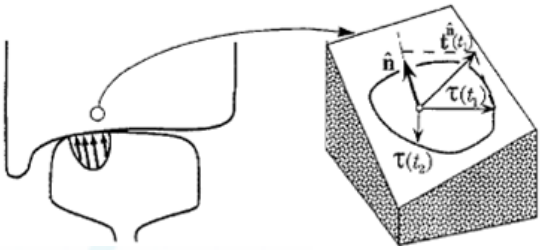

Figure 5: Equivalent stress approach

Concept of Damage

It is postulated that damage takes place during the time portions when the inequality (1) is fulfilled. In order to quantify the damage, a Wohler curve is employed. By use of this curve, the number, Nt, of stress cycles to failure for the current magnitude of loading can be found. The corresponding damage is defined as Dt = 1 / Nt, which, after some manipulations,

$$D_t = 10^{5(\tau e - \tau EQt)/(\tau e - \tau f) - 6} \quad \text{---------- (2)}$$

Where, D_t = is the damage corresponding to the current equivalent-stress.

l = is the number of the current stress cycle

τ_f = is the ultimate stress in pure shear

τ_{EQt} = is the current equivalent-stress

Predictive Model for Rolling Contact Fatigue

1. For Surface initiated fatigue

A fast and reasonably accurate way of identifying load levels corresponding to surface fatigue in rolling contact is the use of shakedown maps, Such a diagram uses the following input parameters.

The yield stress in pure shear (torsion), k

Vertical load magnitude, Fz

Llateral load magnitude, Flat
Semi-axes of the Hertzian contact, a and b

The vertical load magnitude, contact geometry and the yield stress in shear, forms a normalized vertical load.

$$v = \frac{3Fz}{2\pi abk} = \frac{Po}{k}$$

which is combined with the utilized friction coefficient, defined as

$$\mu = \frac{F_{lat}}{F_z} = \frac{\sqrt{F_x^{\,2} + F_y^{\,2}}}{F_z}$$

Here, F_X and F_Y are lateral loads in the wheel–axle and rail direction. These measures define a work point (μ,ν) in the shakedown map. The equation of boundary curve for surface flow in the shakedown map,

$$v = 1/\mu$$

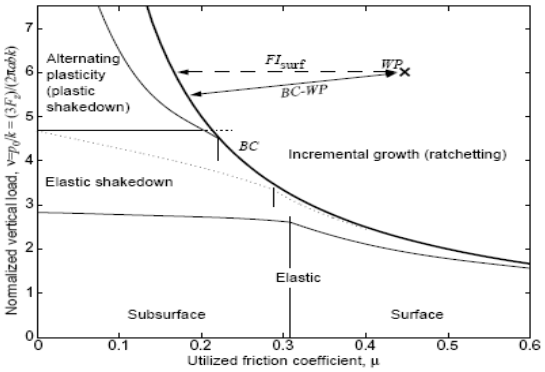

Figure 6: Normalized Force Vs Friction

In a proportional plot, BC is almost vertical. Hence, the surface fatigue index is taken as the horizontal projection of the shortest distance between BC and the current WP positive if WP is to the right of BC). The fatigue index is thus given by

$$FI_{surf} = \mu - \frac{1}{v} = \mu - \frac{2\pi abk}{3F_z}$$

Surface fatigue is predicted to occur if,

$$FI_{surf} > 0$$

2. Subsurface Initiated Fatigue

This type of fatigue has been analyzed by means of numerical simulations employing the Dang Van multiaxial fatigue initiation criterion recalled as,

$$\sigma_{EQ} = \max_t[\sigma_{EQ}(t)] = \max_t[\tau_a(t) + a_{DV}\sigma_h(t)] > \sigma_e$$

Here,$\tau_a(t)$ is the time-dependent shear stress 'amplitude'. Details on the derivation of $\tau_a(t)$ are, for instance, Further,a_{DV} is a material parameter, $\sigma_{h(t0)}$ is the hydrostatic stress positive in tension) and σ_e is the equivalent fatigue limit. The fatigue index proposed in the current model is an approximation (based on the assumption of Hertzian contact) of the magnitude of the largest subsurface Dang Van equivalent stress,

$$FI_{sub} = \frac{Fz}{4\pi ab}(1+\mu^2) + a_{DV}\sigma_{h,res}$$

According to the Dang Van criterion, fatigue damage will be predicted by the inequality

$$FI_{sub} > \sigma e$$

Here, σ_e is the equivalent fatigue limit (normally taken equal to the fatigue limit in pure shear).

3. Fatigue initiated at deep defects

The fatigue impact at the defect is fairly unaffected by the contact geometry at moderate vertical load magnitudes. This motivates adopting the vertical load magnitude as 'fatigue index'

$$FI_{def} = F_z$$

This index can be employed to compare the relative impact of different train/track configurations presumed the wheel material is unaltered. For a quantitative prediction, fatigue is predicted by the following inequality

$$FI_{def} > F_{th}(z, d, H, ...)$$

It is, today, known that F_{th} is a function of the position of the defect below the wheel tread **z** , the size of the defect d , and of load history, H. It is also likely that F_{th} depends on shape and metallurgical composition of the defect.

4. Dang Van Criteria

In a multiaxial state of stress, the fatigue behavior is more complicated. The state of stress is now defined, not by one, but by six components (in the general case). In order to quantify the fatigue impact under such a state of stress, an equivalent scalar stress measure is normally adopted. Such an equivalent stress can be based on an energy measure compare with the von Mises effective stress). Fatigue criteria of this type are the Sines criterion and the Crossland criterion. Alternatively, a measure based on the stress history projected on a critical plane (compare with the Tresca effective stress) can be used. An example of such a criterion is the Dang Van criterion, which has been adopted in the present thesis and which will now be described. The Dang Van criterion defines an equivalent stress as a combination of the fluctuation of the shear stress from its mid value during a stress cycle and the hydrostatic stress (taken positive in tension). It states that fatigue damage will occur if the inequality.

$$\sigma_{EQ,DV}(t) = \tau a(t) + a_{DV}\sigma h(t) > \sigma e$$

is fulfilled during some part(s) of a stress cycle. Here, σ_e is the equivalent fatigue limit and a_{DV} a material parameter. This relationship is graphically represented *in figure.*

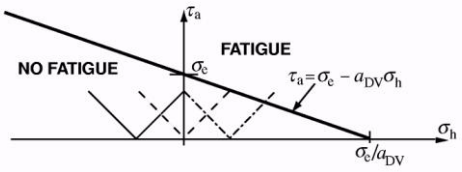

Figure 7: Dang Van criteria

$$\tau_{max}(t) + a_{DV}\sigma_H(t) = \tau_W$$

with a_{DV} being a constant to be determined, τ_W the fatigue limit in reversed torsion, $\sigma_{H(t)}$ the instantaneous hydrostatic component of the stress tensor and $\tau max(t)$ the instantaneous value of the Tresca shear stress,.

$$\tau_{max}(t) = \frac{\hat{s}_I(t) - \hat{s}_{III}(t)}{2}$$

evaluated over a symmetrized stress deviator, which is obtained by subtracting from the stress deviator.

$$S_{ij}(t) = \sigma_{ij}(t) - \delta_{ij}\sigma_H(t)$$

a constant tensor, $S_{ij,m}$ i.e.

$$\hat{s}_{ij}(t) = s_{ij}(t) - s_{ij,\mathrm{m}}$$

$$\max_t[(S_{ij}(t)-S_{ij},m)(S_{ij}(t)-S_{ij},m)] = \min_{Sij}\max_t[(S_{ij}(t)-S_{ij})(S_{ij}(t)-S_{ij})]$$

If we consider a material imperfection as a small crack, its influence on the fatigue resistance in uniaxial loading can be graphically representated by a so-called Kitagawa-Takahashi diagram, see *figure.* Here, the solid line shows the threshold stress magnitude for fatigue failure of the component. It is seen that if a material defect is small enough, it will have no influence on the fatigue resistance (with respect to experimentally found fatigue limits for unnotched and polished test samples). Further, for geometrically long defects, there exists a threshold stress intensity range, AAT_{th}, which is independent of the defect size. Combinations of stress amplitudes and defect sizes between the dashed and the solid line will initially make the cracks propagate. They will, however, come to an arrest at crack sizes corresponding to the intersection with the solid line.

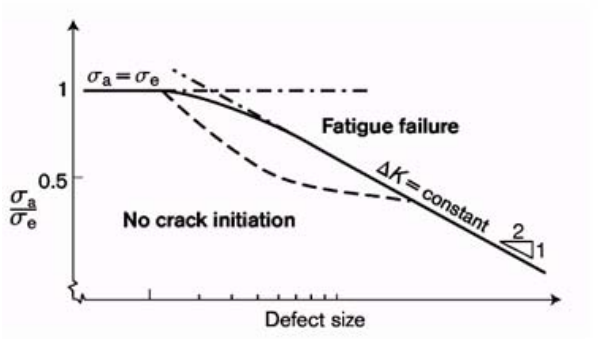

Figure 8: Kitagawa-Takahashi diagram

5. Results discussion from previous studies

J.W. Ringsberg, M. Loo-Morrey, B.L. Josefson, A. Kapoor, J.H. Beynon in in their paper "Prediction of fatigue crack initiation for rolling contact fatigue" carried out FEM simulation of railwheel contact. The simulation results using the FE model were presented for elastic shakedown, plastic shakedown and ratcheting material responses. At ratcheting material response, the results from the FE simulations are compared with the results from the ratcheting model. The simulated combinations of contact pressure and friction coefficient are presented. In the shakedown map, regions for different material responses (elastic, elastic shakedown, plastic shakedown, ratcheting) are presented dependent on the combination of the load factor ***Po/k*** and the friction coefficient μ .

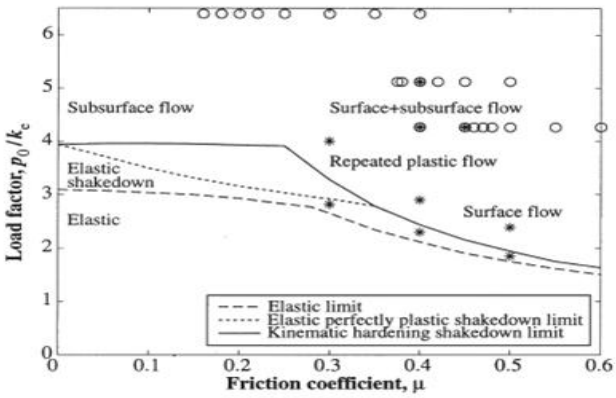

Figure 9: Shakedown map

Jonas W. Ringsberg , Torbjorn Lindba¨ck in their paper" Rolling contact fatigue analysis of rails including numerical simulations of the rail manufacturing process and repeated wheel rail contact loads" carried out simulation of manufacturing process of rail wheel.

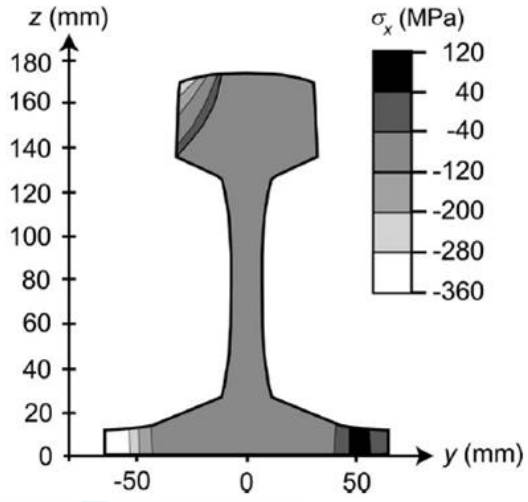

Figure 10: rail longitudinal residual stress distribution after cooling

Parametric Studies

1. Wheel diameter

The diameter of the wheel will affect the fatigue damage. One simple explanation is that the radius of the wheel will affect the internal stress in the wheel according to the Hertz theory.

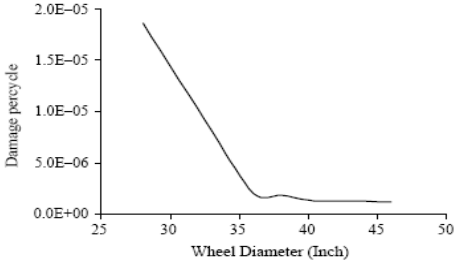

Figure 11: Damage Vs Diameter of wheel

2. Vertical Loads

The damage accumulation rate on the wheel section for the 0.914 m (360) wheel under different vertical loads (64 KN, 96 KN, 128 KN, 160 KN and 192 KN) are calculated and plotted.

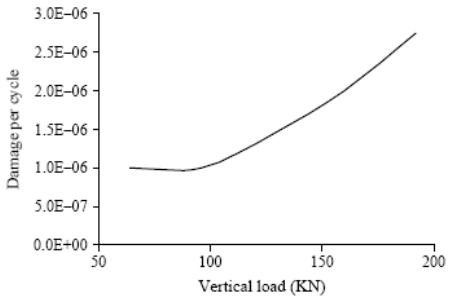

Figure 12: Damage Vs vertical load

3. Hardness of Material

Damage accumulation rate increases as the hardness increases, this is because material with higher hardness, the local plastic flow at the contact surface is not likely to occur and a smaller contact area between wheel and rail is obtained

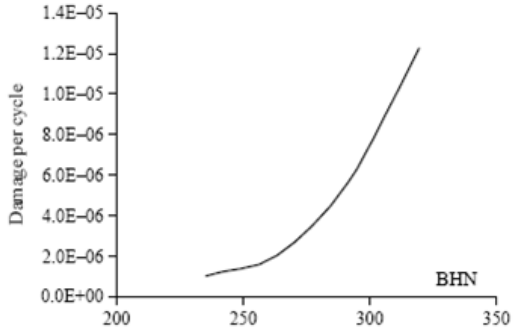

Figure 13: Damage Vs Hardness

4. Fatigue Strength

The fatigue damage accumulation rate decreases as the material fatigue endurance increases as expected. In this case, no crack will be initiated if the fatigue endurance limit is higher than 340 MPa

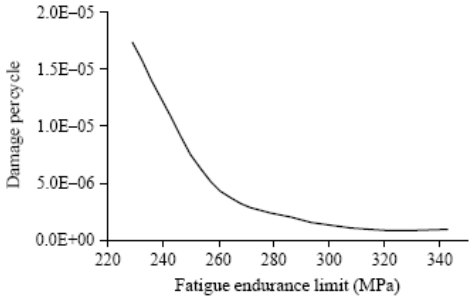

Figure 14: Damage Vs Endurance limit

References

[1] P.J.Mutton "ROLLING CONTACT FATIGUE OF RAILWAY WHEELS UNDER HIGH AXLE LOAD " MONASH UNIVERSITY (2001)

[2] P.J.Mutton, C.J.Epp and J.Dudek "Rolling contact fatigue in railway wheels under high axle loads " Wear, 144 (1991) 139-152

[3] Anders Ekberg "Rolling contact fatigue of railway wheels" CHARMEC Department of solid mechanics

[4] G. Donzella , M. Faccoli , A. Ghidini , A. Mazz_u , R. Roberti "The competitive role of wear and RCF in a rail steel " Engineering Fracture Mechanics 72 (2005) 287–308

[5] S. BogdaAski, M. Olzak, J. Stupnicki "Numerical stress analysis of rail rolling contact fatigue cracks " Wursuw University of Technology. Institute of Aeronautics, ul. Nowowiejske 24, 00-665 Warsaw, Poland

[6] Eka Lansler, Elena Kabo "Subsurface crack face displacements in railway wheels" Wear 258 (2005) 1038–1047

[7] Jonas W. Ringsberg , Torbjorn Lindba "Rolling contact fatigue analysis of rails inculding numerical simulations of the rail manufacturing process and repeated wheelrail contact loads" International Journal of Fatigue 25 (2003) 547–558

[8] Anders Ekberg, Elena Kabo "Fatigue of railway wheels and rails under rolling contact and thermal loading—an overview " Wear 258 (2005) 1288–1300

[9] Y.B. Guo,_, Mark E. Barkey "Modeling of rolling contact fatigue for hard machined components with process-induced residual stress" International Journal of Fatigue 26 (2004) 605–613

[10] Stanisław Bogdanski , Michael W. Brown "Modelling the three-dimensional behaviour of shallow rolling contact fatigue cracks in rails " Wear 253 (2002) 17–25

[11] Anders Ekberg , Peter Sotkovszki "Anisotropy and rolling contact fatigue of railway wheels " International Journal of Fatigue 23 (2001) 29–43

[12] Jonas W. Ringsberg "Life prediction of rolling contact fatigue crack initiation " International Journal of Fatigue 23 (2001) 575–586

[13] S. BogdaAski, M. Olzak, J. Stupnicki "Numerical stress analysis of rail rolling contact fatigue cracks " Wear 191 (1996) 14-24

[14] A. Ekberg "Rolling contact fatigue of railway wheels—a parametric study " Wear 211 (1997) 280-288

[15] J.W. Ringsberg , M. Loo-Morrey , B.L. Josefson , A. Kapoor , J.H. Beynon "Prediction of fatigue crack initiation for rolling contact fatigue " International Journal of Fatigue 22 (2000) 205–215

[16] M.S raml , J. Flasker, I. Potrc " Numerical procedure for predicting the rolling contact fatigue crack initiation " International Journal of Fatigue 25 (2003) 585–595

[17] Elena Kabo, Anders Ekberg "Material defects in rolling contact fatigue of railway wheels—the influence of defect size " Wear 258 (2005) 1194–1200

[18] H. Desimone , A. Bernasconi, S. Beretta "On the application of Dang Van criterion to rolling contact fatigue " Wear 260 (2006) 567–572

[19] Yongming Liu, Brant Stratman, Sankaran Mahadevan "Fatigue crack initiation life prediction of railroad wheels " International Journal of Fatigue 28 (2006) 747–756

[20] Jonas W. Ringsberg, Francis J. Franklin, B Lennart Josefson, Ajay Kapoor, Jens C.O. Nielsen "Fatigue evaluation of surface coated railway rails using shakedown theory, finite element calculations, and lab and field trials " International Journal of Fatigue 27 (2005) 680–694